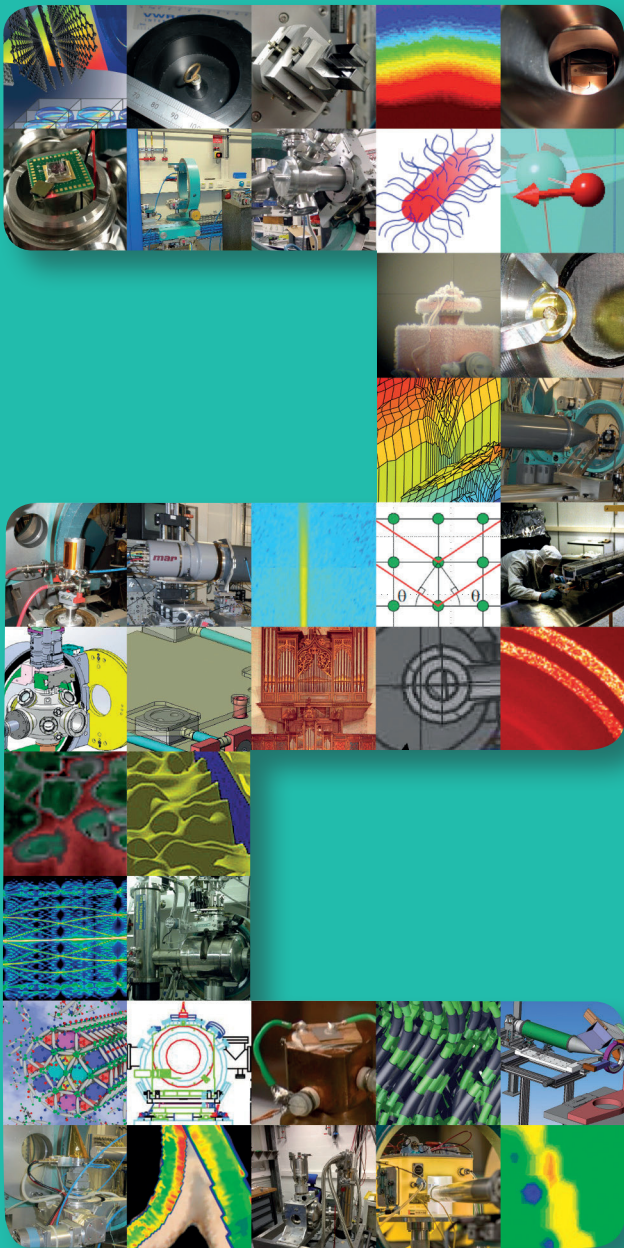


XMAS

NEWSLETTER

2017



YEARS



XMaS News

CONTENTS

2 XMaS News

3 Collaborative Projects

4 Workshops

6 Beamline Developments

8 Condensed Matter

12 Materials Science

13 Soft Matter

14 Energy & Catalysis

16 Access to offline facilities

*On the cover:
20 years of science
and instrumentation
on XMaS.*

As you will see on pages 4 and 5 of this Newsletter, we have recently celebrated the 20th anniversary of operations. We thank all of our users for helping to grow and diversify the scientific challenges that are tackled on the beamline and, crucially, for contributing to the development of the current vibrant user community. All of the past newsletters are online, so if you are feeling nostalgic please take a look back in time!

The engagement and support of our users are crucial if the XMaS beamline is going to continue into the future. To begin this process, a “Statement of Community Need” was submitted to EPSRC during the summer of 2017. This document was well received, although the application process for further funding is still ongoing and subject to final peer review approval. With the future in mind we are beginning to prepare the XMaS facility for the EBS upgrade with a new lead door already installed on the beamline and close to the optics hutch. Major upgrades in detectors, sample environments, data control and reduction as well as upgrades in operational capability are planned for the dark period of 2019. A new double toroid mirror system to cover the enhanced energy range from 2 to 33 keV is now out for tender. The biggest impact to user operations is the necessity to extend the experimental hutch to accommodate the new source position in the upgraded storage ring. The experimental hutch will be extended into the current control area by some four metres. This will begin in the middle of May, with reduced operations in that operating cycle. For this reason priority will be given to experiments required for students’ PhD studies and any hot topics in the next proposal round. We will be issuing a special call for this allocation period and ask in advance for your understanding as we upgrade the beamline components and capabilities. More details can be found on pages 6 and 7.

The offline facilities, which include a Cu laboratory x-ray micro source as well as the magnetic and electrical characterisation laboratory, exploit the range of sample environments that are available and accessible for users. We look forward to

receiving your proposals for either onsite or remote access projects and encourage you to think how you could use these facilities during the dark period.

During this past autumn the beamline was evaluated by the ESRF in its fourth quinquennial review. The panel was “truly impressed by the dedication, enthusiasm and technical skills of the beamline staff” and we would like to echo those comments here and thank the beamline staff for all of their hard work. The panel noted the “impressive development of dedicated set-ups and sample environments” and the work on “flexible and combinatorial sample environments”. This has traditionally been a strength of the beamline, and is driven by the interactions that the beamline team has with the user community. We would like to take this opportunity to thank the ESRF and the review panel for their efforts and helpful comments. We encourage you to get in contact with us if there are experiments you want to do that need some modifications or design work for new sample environments, techniques or operational control. We are also particularly interested in expanding our link to industry and will be working on this strategy during 2018/9. For those who might be interested, there is now a promotional video of the beamline which can be viewed on our web site [1] and on YouTube [2]. Please feel free to use it in any of your presentations to advertise the facility.

The “XMaS Scientist Experience” goes from strength to strength with the visit of the successful winners in 2017 to XMaS and the ESRF during July 2017. Once again we are indebted to the Synchrotron@School program [3, 4] and the generosity of the ESRF in making this national competition the success it is and providing an opportunity to encourage young women into science. We have already launched the 2018 competition [5]. If you know anyone who meets the application criteria please encourage them to apply.

The XMaS@20 meeting held at the ESRF was a great success and it was good to see so many people there with many old friends and colleagues. We thank Huber GmbH for sponsoring the event. The next

user meeting will be held in the UK sometime in the early summer where it is hoped that details of the new (post EBS) XMaS facility will be presented.

We would like to take the opportunity of this newsletter to congratulate Bill Stirling who has recently been awarded the prestigious title of Companion of the Order of St Michael and St George for services to British science and international science collaboration [6]. Finally we note that Kayleigh Lampard has taken up another role at the University of Warwick. We would like to thank Kayleigh for all of the work that she did as the project administrator

at Warwick, particularly for her central role in the XMaS Scientist Experience. We wish her all the best for the future and welcome Natacha Borrel as the new project administrator.

Chris Lucas, Tom Hase and Malcolm Cooper

- [1] www.xmas.ac.uk/xmasbeamline/
- [2] <https://www.youtube.com/watch?v=AJcLjBRxTvc>
- [3] www.esrf.fr/home/education/synchrotronschool.html
- [4] <https://www.youtube.com/watch?v=U6HDiVBj4Tw>
- [5] <https://tinyurl.com/y7ykdqjh>
- [6] <https://www.thegazette.co.uk/notice/2937702>

Collaborative Projects

Metrology for advanced energy-saving technology in next-generation electronics applications - ADVENT

M.G. Cain, Electrosiences Ltd – for more information contact M.G. Cain, Electrosiences Ltd, UK or P. Thompson, XMaS, ESRF, France.

markys.cain@electrosiences.co.uk
pthomps@esrf.fr

XMaS and Electrosiences Ltd are major partners in a new European Research Project – ADVENT.

Improved power and material measurements will enable development of optimised, future-proof electronic devices.

The roll-out of 5th generation (5G) telecommunications across Europe by 2020, and the emergence of the Internet of Things (IoT) with 50 billion connected devices, will significantly increase energy demand due to the continuous power consumption of the electronic devices needed to deliver these technologies. Development of novel ultra-low power devices (**Fig. 1**) which support the sustainable adoption of these technologies requires traceable measurement techniques for the characterisation of advanced materials and components, and for the generation of reliable and accurate data for efficient power management systems.

This EURAMET* project will provide such traceable measurements of power, power losses and emerging electronic materials properties, to aid the development of new materials and more efficient electronic components. The results will enable European industries to optimise devices and systems designed for 5G and IoT applications requiring ultra-low power, more energy efficient operation.

Participating EURAMET NMIs** and DIs***

- Bundesanstalt für Materialforschung und – Prüfung, BAM (Germany)
- Czech Metrology Institute, CMI (Czech Republic)
- Justervesenet - Norwegian Metrology Service, JV (Norway)
- Laboratoire national de métrologie et d'essais, LNE (France)
- Federal Institute of Metrology METAS, METAS (Switzerland)
- National Physical Laboratory, NPL (United Kingdom)
- Physikalisch-Technische Bundesanstalt, PTB (Germany)

Other Participants

- Centre National de la Recherche Scientifique, CNRS (France)
- Electrosiences Ltd (United Kingdom)
- University of Liverpool (United Kingdom)
- Universitat Politècnica de Catalunya (Spain)
- Université des Sciences et Technologies de Lille - Lille I (France)
- Université Paris-Est Marne-la-Vallée (France)
- University of Surrey (United Kingdom)

The role of XMaS is to develop tools allowing high frequency dynamic x-ray diffraction in thin films and *in-situ* strain characterisation of bulk ferroelectric materials. The project started on 1st September 2017 and will run for three years. More information as well as the 'publishable summary' of this project (n°16ENG06) can be found on the EURAMET website [1].

- [1] <https://tinyurl.com/yaccznyr>

* EURAMET: The European Association of National Metrology Institutes

** NMIs: National Metrology Institutes

*** DIs: Designated Institutes

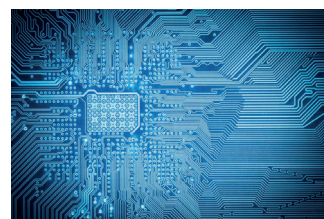


Fig. 1: New nanoscale electronics for low power RF applications.

XMaS celebrating its 20 years of user operation

To celebrate its 20 years of user operation, the UK-CRG beamline (BM28) organised a rather special user meeting, called “XMaS@20” which took place at the ESRF on the 20-21 September 2017.

XMaS was born back in 1992 with Bill Stirling and Malcolm Cooper (Fig. 2) as its parents, each being a professor at the Universities of Keele and Warwick, respectively. The official opening of the beamline was celebrated on the 19th September 1997 in the presence of the vice-chancellors of the Universities of Warwick, Keele and Liverpool. Stuart Ward the representative of EPSRC*, our funding council since the very beginning, was also there. XMaS has been in fact “the joint longest running facility funded by EPSRC, being one of the first to move from



Fig. 2: The co-origins of the XMaS beamline, Bill Stirling (left) and Malcolm Cooper (right).

a general grant to facility status” as was noted by Simon Crook our EPSRC contact until very recently. In total EPSRC has invested around £19M over the four operational phases of the beamline. After the initial 3-year construction phase, the first user group led by Ted Forgan (University of Birmingham) arrived on the beamline in April 1998. Ted has remained a regular user of the beamline ever since.

Obviously the major part of the XMaS family resides in the UK, but members can be found all around the world, e.g. France, Spain, Germany, Sweden but also in the USA, Canada, Brazil, Russia, Iran, etc. Around 60 delegates gathered at the ESRF in a very friendly atmosphere to listen to a variety of presentations starting from a description of XMaS from the early days, when it was mainly dedicated to studies of magnetic materials to talks covering the broad and more recent research portfolio of the beamline.

For those who did not know, the acronym XMaS meaning X-ray Magnetic Scattering, was chosen at a time when the beamline was mainly dedicated to studies of magnetic materials. Over the years XMaS has evolved to meet the needs of a broader interdisciplinary user community (Fig. 6) and has thus become a beamline for material scientists more generally. Nowadays, the same acronym can be used, but now stands for X-ray Materials Science. Don't get us wrong though, we still have physicists looking at superconductors, magnetic thin films and even uranium based samples! Today, in addition, we have users searching for novel functional materials to be used in the next generation of photovoltaics, transistors and also users more interested in how



Fig. 3: Some of the XMaS@20 attendees during a coffee break in the ESRF central building.



Fig. 4: Robert Cernik in the difficult job of giving the after dinner talk at the restaurant Fantin Latour.

nanoparticles could be utilised without detrimental effects on our body. Who would have thought 20 years ago that scientists would come to XMaS to explore teeth, bones and how copper ions act as contraceptive in an intra uterine device? Experiments aiming to understand corrosion mechanisms in cultural heritage artefacts or even in nuclear waste also happen at XMaS on a regular basis. If you pop along the beamline, don't be surprised to see chemists looking at new ways of improving catalysts

and batteries for making your cars cleaner. Over this 2-day meeting, we heard stimulating and lively reports on all of those different disciplines, but it was also so nice to see old colleagues and friends.

We would like to thank STFC** for having generously offered to support the coffee breaks and Huber Diffractionstechnik GmbH [1] for sponsoring the overall event. Of course a big thank you to EPSRC for making this very special conference possible. For those who could not make it, the conference booklet and all the pictures can be viewed on our web site [2]. A video captured during the conference is also available on YouTube [3]. So now why not XMaS@30 or 40! Who knows how far into the future the facility will be supporting users. Once again, thanks to everyone who made the meeting such a success.

[1] <http://www.xhuber.de/en/home/>

[2] www.xmas.ac.uk/impact/meetings/xmas_20/

[3] <https://www.youtube.com/watch?v=tKtY7f8UPTw>

* EPSRC: Engineering and Physical Sciences Research Council

**STFC: Science and Technology Facilities Council



Fig. 5: Nice to catch up with people during the coffee breaks.

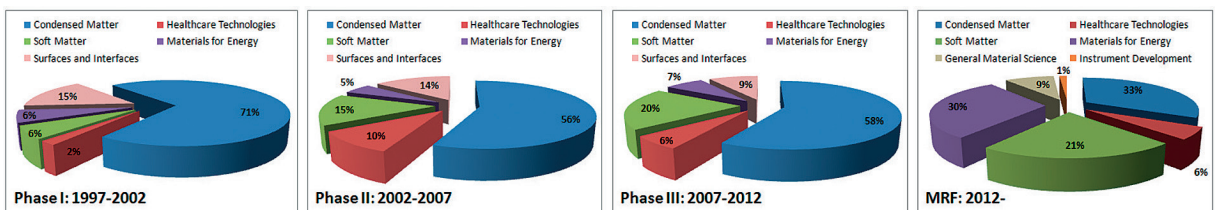


Fig. 6: Evolution of the research portfolio on XMaS through the four operational phases.

XMaS looking into the future

The ESRF has launched an ambitious programme to upgrade the existing storage ring lattice for an Extremely Brilliant Source (EBS [1]). In this context, the XMaS user community has identified a clear need to expand capabilities to address the current and future challenges across the research portfolio. After 20 years of operation, assuming XMaS is funded, we will make strategic use of the ESRF dark period (December 2018 - August 2020) to undertake timely upgrades to our infrastructure, replace critical components and commission new controls ensuring full operational capability when user operations of the new storage ring restart. The capital investment plan ensures competitive viability for the next 10 to 15 years and has been prioritised by our users and management committee.

A new source

We will upgrade our current source to a high field 0.86 T short bend magnet. This proposal was contained in a Conceptual Design Report (CDR) presented to the ESRF Strategic Advisory Committee, which fully approved the CDR. The higher magnetic field increases the available flux at energies above 20 keV by several orders of magnitude. Geometrically the source point will move 2.78 m upstream and the x-ray beam 10 cm closer to the ring at the monochromator position.

A new mirror system

The upgrade of the current mirror system becomes necessary to benefit fully from the upgraded source characteristics. The new system will comprise two interchangeable, meridionally bendable, cylindrical mirrors (coated with chromium and platinum, respectively) to focus the new source onto the sample position. The new spot size (H x V) at the sample position will be significantly smaller (50 x 120 μm^2) than the current focused spot size (300 x 600 μm^2), with higher flux density. Studies on smaller samples or on localised regions of larger samples will thus be boosted.

The double mirror system will increase the working cut-off energy up to ~33 keV (15 keV today). It will be possible to probe the same sample volume while keeping the same experimental conditions between low energies and high energies by translating the focusing mirror to the appropriate mirror coating (see Fig. 7). This ~33 keV cut-off energy allows experiments to access the K edges of the rare earths as well as enabling new studies on the L edges of the transuranic elements (exploiting XMaS's operational licence). Furthermore, access to the K edges from

Ru through to I will open a new range of experiments on new catalysts and green chemistry. The higher energies will also facilitate experiments on buried interfaces in more complex sample environments and studies of solid-liquid interfaces relevant to electrochemical processing. Research beyond 33 keV will still be possible with reduced flux (Fig. 7). The call for the mirror tender is now out.

A new monochromator

The current water cooled double-bounced Si(111) monochromator will be replaced by cryogenically cooled crystals to overcome the present problem of heat load. The new design will expand our energy range down to 2.05 keV. The spectroscopy community will also greatly benefit from the installation of a new monochromator driver, which will allow a rapid and continuous scanning of the energy.

A longer experimental hutch

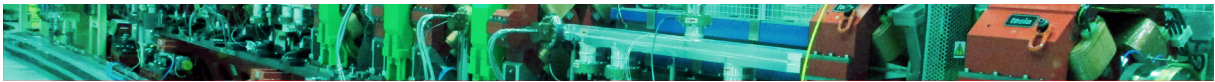
The experimental hutch will be extended by 4 m occupying the space of the present control cabin to accommodate the new source position in the upgraded storage ring. The control cabin will subsequently move 4 m back too and be located close to the offline x-ray source facility. The longer hutch will allow the diffractometer to be moved back by ~3 m to maintain a magnification close to 1 and minimise optical aberrations. The construction work will start in May 2018 and finish in September 2018. Additional beam defining and conditioning elements (e.g. in-vacuum phase-plates permanently mounted) will be incorporated increasing our operational efficiency and allowing rapid switching between experimental configurations and higher user throughput.

SAXS experiments will also greatly benefit from the hutch extension. The maximum sample-to-detector distance will extend to ~2.6 m (~1.5 m today) allowing access to smaller Q-values ~0.012 \AA^{-1} (0.02 \AA^{-1} today) corresponding to real space length scales ~ 52 nm (30 nm today). These improvements could be beneficial for SAXS experiments using strong magnetic fields too (see a current example by Zeng *et al.* page 13).

The Huber diffractometer will also be refurbished and the 2Θ arm made stiffer for heavier detectors to be mounted.

New sample environment

New gas and liquid handling systems have been identified by users as critical for *in-operando* studies. For spectroscopy experiments, a reliable incident x-ray beam monitor (e.g. ionisation chamber, IC) is crucial and needs to be optimised for each energy. This is normally performed by manually opening and



closing valves to change the gas in the IC, which can lead to a significant time overhead. During the upgrade, the IC gas handling will be automated instead, which will be important for time dependent reactions. Additionally, the gas handling system will be designed to deliver safely toxic/flammable gasses to the sample environment routinely used for catalysis experiments. The system will be permanently mounted outside the experimental hutch.

New detectors

We will invest in a new suite of detectors as the efficiency of Si-based systems degrades above 18 keV. Our detectors will include a Pilatus CdTe 100k for high energies and spectroscopic studies will be supported by a multi-element energy dispersive detector and fast MCA card. The current MAR CCD camera will be replaced with a Pilatus 1M-S. A small Eiger 500k detector with 2 μ s readout time will facilitate dynamic experiments.

New control software and data processing

Operationally, the beamline needs to be robust and efficient with control and core systems upgraded to maintain ESRF standards. To facilitate rapid configurational changes, the SPEC sessions will be consolidated and refined. The beamline will run in pseudo six-circle (PSIC) geometry. Enhanced data pipeline for data visualisation and refinement will ensure smoother user operations and more rapid impact and dissemination. Recent efforts have concentrated on data reduction, visualisation and processing (e.g. esaProject [2]). It will be important to improve such provision as well as update our

control protocols during the upgrade to maximise the research output of the beamline.

The offline facilities will be available for users during the dark period but will be run only by the XMaS staff.

To prevent our user community from being too adversely affected by the ESRF shutdown in 2019 we are ensuring our offline facilities are fully operational. Beamline staff may have to handle remote, or “mail in” requests as user access to the ESRF will likely to be restricted during commissioning.

[1] www.esrf.fr/about/upgrade

[2] www.xmas.ac.uk/other_projects/esaproject/

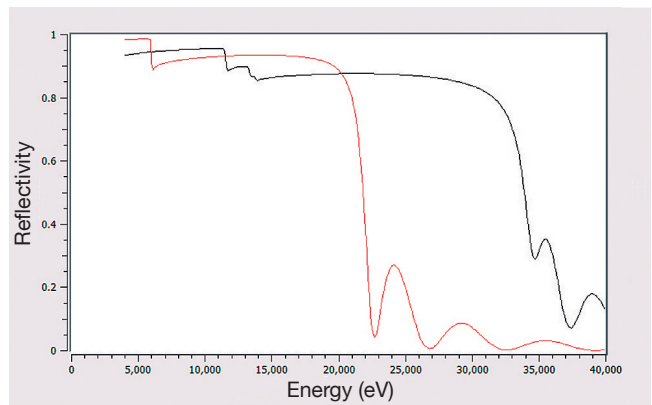


Fig. 7: Reflectivity profile of the Cr (red) and Pt (black) coated stripe of the new XMaS toroidal mirror system as a function of energy.

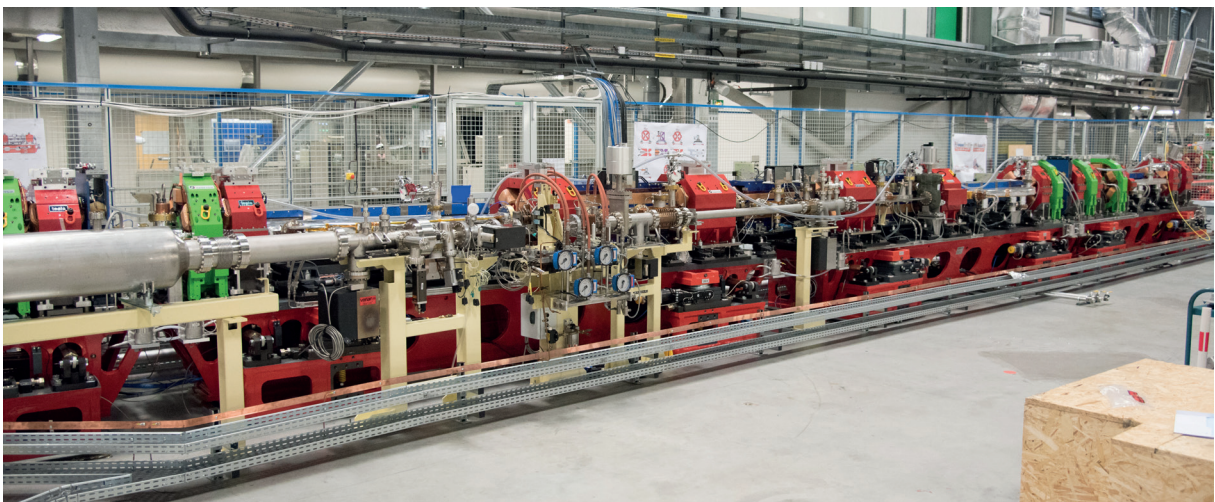


Fig. 8: The EBS mock-up cell consisting of girders, magnets, vacuum chambers and other components being assembled in the ESRF's Chartreuse hall. Courtesy of C. Argoud.

Atypical band gap temperature dependence in solar cell material

M. Birkett, C. Savory, P. Thompson, T. Veal, et al. – for more details contact M. Birkett, Stephenson Institute for Renewable Energy, Dept. of Physics, University of Liverpool, UK.

m.birkett@liv.ac.uk

Photovoltaics (PV) research seeks low cost, nontoxic and earth-abundant materials with desirable properties for solar cells: an optimal band gap, strong absorption, little non-radiative recombination and favourable carrier dynamics. Our group studied the band gap temperature-dependence and thermal expansion in the candidate PV absorber Cu_3N by Fourier transform infrared spectroscopy (at Liverpool), x-ray diffraction (XRD) between 4.2 and 100 K at the **XMaS offline x-ray source facility** (Grenoble), and by first-principles calculations (at University College London).

Temperature-dependent XRD studies are especially valuable for several reasons:

1. Band gaps depend on temperature due to lattice expansion, electron-phonon interactions and potential phase transitions [1].
2. Solar-cell performance may be impacted significantly by band gap changes between ambient and operating temperatures: with efficiencies falling by as much as 0.1%/K [2].
3. Crystal interfaces and band alignments may depend on thermal expansion.

Cu_3N has a rather open, anti- ReO_3 (perovskite-like) structure (space group $Pm3m$), leaving substantial room to accommodate structural distortions or



impurities. Negative thermal expansion (increasing volume with decreasing temperature) is predicted for Cu_3N , while the anti- ReO_3 structure is also associated with novel zero-thermal expansion materials. XRD work was therefore commenced to evaluate the role of thermal expansion in Cu_3N and to assess possible phase transitions.

This work found a direct gap of 1.68 eV at 300 K with atypically small temperature dependence and desirably strong absorption. The band gap redshifted by just 24 meV between 4.2 and 300 K (100 meV is more typical). The lattice parameter was fit with the quadratic function $1.01(11)\times 10^{-7} T^2 - 1.1(3)\times 10^{-5} T + 3.81807(22) \text{ \AA}$ (Fig. 9). The lattice specific heat capacities C_V were found to be 43 and 300 $\text{J kg}^{-1} \text{K}^{-1}$ at 100 K and 300 K, respectively.

This work also suggested that the electron-hole interaction may contribute significantly to optical absorption in Cu_3N and that the material may be suited for applications requiring a largely temperature-invariant band gap [3].

- [1] J. Bhosale et al., Phys. Rev. B 86, 195208 (2012).
 [2] P. Singh et al., Sol. Energy Mater. Sol. Cells 101, 36 (2012).
 [3] M. Birkett et al., Phys. Rev. B 95, 115201 (2017).

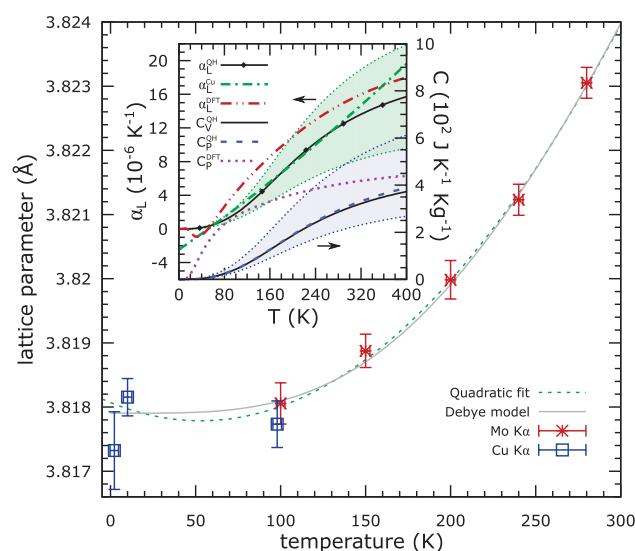
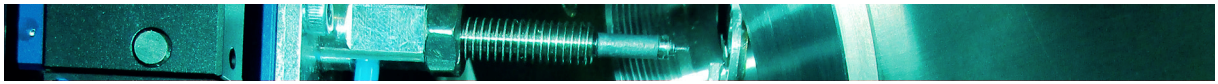


Fig. 9: Plots of cubic lattice parameters fit by Pawley refinement, with the lattice parameter evolution fit by a quadratic and a quasiharmonic Grüneisen-Debye-Einstein model. The inset compares the quasiharmonic (QH) thermal linear expansion α_L and heat capacities C_V and C_P with those from first-principles calculations (α_L^{DFT} and C_P^{DFT}) and from a cubic fit (α_L^{Cu}). The filled regions around α_L and C_V denote the uncertainties, which are dominated by the Grüneisen parameter uncertainty. Negligible thermal expansion is seen below 100 K.



Low temperature ferroelectric behaviour in morphotropic $\text{Pb}(\text{Zr}_{1-x}\text{Ti}_x)\text{O}_3$

J.B.J. Chapman, O.T. Gindele, C. Vecchini, P. Thompson, M. Stewart, M.G. Cain, D.M. Duffy, A.V. Kimmel – for more information contact J.B.J. Chapman, University College London, UK.

jacob.chapman.13@ucl.ac.uk

Functional ferroelectric ceramics are utilised as critical components in many technologies which operate in a wide range of conditions. One of the most widely used ceramic materials is lead zirconate titanate $\text{Pb}(\text{Zr}_{1-x}\text{Ti}_x)\text{O}_3$ (PZT), which is a disordered solid solution of PbTiO_3 and PbZrO_3 , used for actuators, transducers, non-volatile memories and micropumps. The morphotropic composition ($0.47 < x < 0.52$) of PZT exhibits the exceptionally high electromechanical response necessary for applications in aeronautic, military and space industries. There have been a number of studies performed at room temperature and above, however the low temperature ($T < 200$ K) properties of PZT are not well characterised.

We studied the effect of temperature on the electromechanical properties and switching behaviour of a near-morphotropic composition of PZT using molecular dynamics (MD) simulations and electrical measurements [1]. Implementing the method developed on XMaS [2], *in-situ* electric polarisation (P-E) hysteresis loops were measured on the XMaS offline sample characterisation facility. The P-E loops were collected under the application of triangular E-field cycles of amplitude 1 kV/mm at a frequency of 0.1 Hz, for temperatures

$80 \text{ K} < T < 300 \text{ K}$ (setup 1). Supplemental measurements were performed at the National Physical Laboratory using a liquid nitrogen bath to measure a thin-film sample of PZT at 77 K with an applied field of 9 kV/mm (setup 2).

The experimental P-E loops were observed to be open square hysteresis curves which widened as the sample temperature was decreased (Fig. 10c). This, necessarily, corresponded to a reduction in the saturation polarisation (P_s) and an increase in coercive field (E_c) (Fig. 10b). However, unlike previous studies which showed that PZT P-E hysteresis loops began to narrow below 160 K, we show that the hysteresis loops continue to widen with decreasing temperature. This discrepancy was identified to be a result of the coercive field exceeding the maximum applied voltage, which prevented the polarisation from switching (Fig. 10d compare to Fig. 10c at 80 K, which used setup 1).

Results from MD simulations of bulk PZT ($x=0.5$) (Fig. 10a, b), using a polarisable core-shell model [3], corroborated our experimental observations. The model was further used to characterise the detailed switching behaviour. It was found that the switching event occurs via a polarisation rotation mechanism at low temperatures, whereas domain nucleation driven switching dominates at room temperature. The success of the simulations provides a robust approach to investigate PZT over the full compositional range and temperatures. It has subsequently been used to identify novel domain morphologies in PbTiO_3 ultra-thin films and intrinsic ageing mechanisms in ferroelectrics [4].

- [1] J.B.J. Chapman *et al.*, J. Am. Ceram. Soc. 101, 874 (2018).
- [2] J. Woodridge *et al.*, J. Synch. Rad. 19, 710 (2012).
- [3] O.T. Gindele *et al.*, J. Chem. Phys. C 119, 17784 (2015).
- [4] J.B.J. Chapman *et al.*, Phys. Chem. Chem. Phys. 19, 4243 (2017); Phys. Rev. Lett. 119, 177602 (2017).

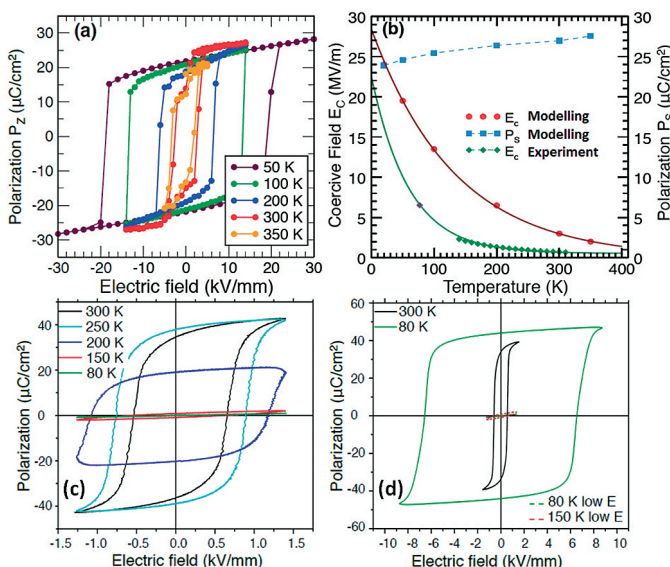
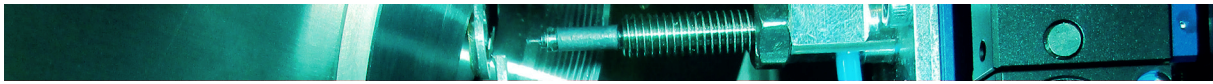


Fig 10: (a) Modelled temperature dependence of the z-component of the polarisation (P_z) with respect to the applied electric field E . With the temperature rise, the shape of the P-E loops evolves from square-like (purple, green, blue) to complex shapes (red and yellow) due to the increased polarisation fluctuation at high temperatures. (b) Temperature dependence of E_c (red) and P_s (blue), both inferred from the P-E loops in (a). Experimental data also plotted in green diamonds with one point in purple diamond (different sample but same composition at 77 K). (c) Measured P-E loops at different temperatures. With the temperature decrease the area of the loops reduces, demonstrating a dielectric-like response. (d) A comparison of 150 K and 80 K loops measured at high (9 kV/mm) and low (1.5 kV/mm) fields. The higher 9 kV/mm field restores the square shaped hysteresis loops.



Large piezoelectricity in electric-field modified SrTiO₃

S. Gorfman, E. Mehner, C. Richter, J. Hanzig, H. Stoecker, T. Leisegang, D.C. Meyer – for more information contact S. Gorfman, Department of Materials Science and Engineering, Tel Aviv University, Israel.

gorfman@tauex.tau.ac.il

Piezoelectricity is the ability of some non-centrosymmetric crystals to transform mechanical and electrical energy into each other. Piezoelectric materials underpin the multi-billion-euro industry of such devices which are used as pressure sensors, actuators and frequency controllers. Despite their great importance, the number of practically useful piezoelectrics (SiO₂, Al_{1-x}Sc_xN and PbZr_{1-x}Ti_xO₃) is limited and the recipes for designing new materials with enhanced piezoelectric coefficients, optimized production costs and suitability for specific applications are continuously being sought.

In this work, we discovered that sufficiently large piezoelectricity can be artificially created in SrTiO₃ (STO) - a material, which is cubic, centrosymmetric and non-piezoelectric under ambient conditions. Our time-resolved x-ray diffraction (XRD) experiments at XMaS and in our home laboratory demonstrated that the previously reported migration-field-induced polar (MFP) phase of STO is strongly piezoelectric, suggesting a new way to “imprint” piezoelectricity in non-piezoelectric materials [1].

According to the procedure described in [2], the MFP-phase of STO is created by exposing the crystal to a static electric field ($E_0 \sim 1$ kV/mm) for a few hours (Fig. 11). It was previously shown [2] that the MFP phase is formed ~ 2 μm beneath the positive electrode, has a tetragonal structure and is pyroelectric. Most interestingly, the MFP-phase is only stable in an electric field: it disappears a few seconds after the electric field is removed.



Fig. 11. The photograph (top) of SrTiO₃ single crystal prepared for the formation of the MFP phase.

To measure the piezoelectric coefficient of the MFP phase we did stroboscopic XRD measurements under an electric field. After forming the MFP phase (by application of 1 kV/mm static electric field), we added an alternating 1 kHz triangular component, which modulated the electric field between 0 and 2 kV keeping the time-averaged value at 1 kV/mm. The response of the bulk STO and the MFP phase was monitored for a selection of Bragg reflections, where the STO/MFP contributions are found at distinct angles. We observed that the bulk STO Bragg peak remains static (sharp and intense peak on the right in Fig. 12), while the MFP phase peak (weak and broad peak on the left in Fig. 12) was shifted linearly with the alternating electric field. Based on the field-dependence of the c-lattice parameter we calculated the related piezoelectric coefficient for different sample thicknesses. The highest piezoelectric coefficient of the MFP phase was found to be 100 pC/N, which is comparable to that of some functional ferroelectric perovskites.

[1] B. Khanbababee *et al.*, Appl. Phys. Lett 109, 222901 (2016).

[2] J. Hanzig *et al.*, Phys Rev B 88, 024104 (2013).

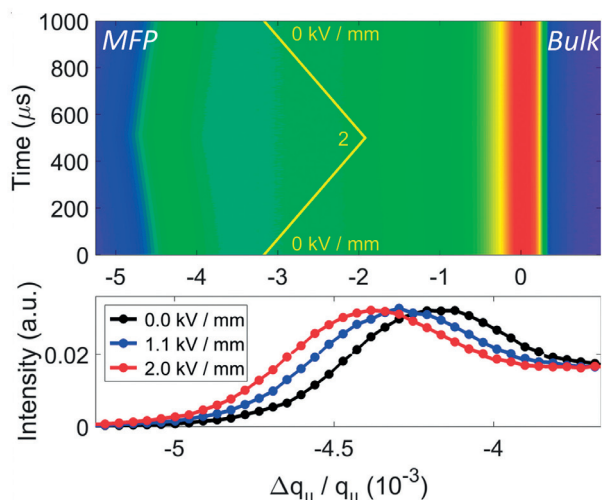
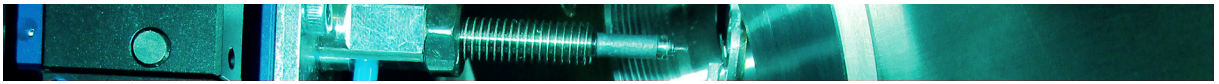


Fig. 12: (top) False-colour maps of time-resolved XRD measured along $q_{||}$ across the (006) Bragg reflection and as a function of electric field. **(bottom)** MFP peak displacement as function of applied field.



Resonant x-ray diffraction reveals the magnetic structure of a heavy fermion superconductor

N. Gauthier, D. Wermelle, J.S. White – for more information contact J.S. White, Laboratory for Neutron Scattering and Imaging, Paul Scherrer Institut, Villigen, 5232, Switzerland.

jonathan.white@psi.ch

In conventional superconductors, electrons form pairs that carry electric charge in the material without dissipation. The electrons are “glued” together through a coupling to the lattice. However, in unconventional superconductors, the pairing mechanism is still elusive and under debate. In heavy fermion compounds superconducting and magnetic phases are often found in close proximity, suggesting that the magnetic degrees of freedom could play a role in the electron glue. An accurate description of the nearby magnetic order is therefore required to deepen our knowledge on these systems.

The Ce-115 compounds $CeMIn_5$ ($M = Co, Rh, Ir$) form an exciting family of heavy fermion materials with a clear interplay between antiferromagnetic and superconducting phases [1]. The ground states of these materials are easily tuned by pressure or chemical doping, making them ideal for investigating quantum critical points and novel phases stabilized by quantum fluctuations. A representative example is $CeRhIn_5$ that has an incommensurate spiral order at ambient pressure [2]. Under pressure, the magnetic order is suppressed and a superconducting state is reached.

We investigated the heavy fermion compound $CePt_2In_7$ that structurally is closely related to the Ce-115 family, with the main difference being a larger spacing of the $CeIn_3$ planes in $CePt_2In_7$. Similar to $CeRhIn_5$, the compound $CePt_2In_7$ is antiferromagnetic at ambient pressure and features superconductivity under pressure where magnetism is suppressed [3]. We performed magnetic resonant x-ray diffraction at XMaS to establish its magnetic structure at ambient pressure. This technique is ideally suited for studying this material in comparison to neutron scattering, where small sample size and neutron absorption are limiting factors.

When compared with the incommensurate antiferromagnetic phases observed in the Ce-115 family, we made the surprising discovery that the magnetic order in $CePt_2In_7$ is described by a commensurate structure with the moments lying in

the basal plane of the tetragonal lattice (Fig. 13a) [4]. The measurements were performed at the Ce L_{II} absorption edge, where the magnetic scattering intensity becomes enhanced due to resonance (Fig. 13b). The magnetic origin of the detected signal was also confirmed by a polarisation analysis (Fig. 13c).

Despite the different types of magnetic order observed, $CePt_2In_7$ and $CeRhIn_5$ both feature an antiferromagnetic order with moments in the basal plane, and similar pressure-dependent phase diagrams. This suggests that the nature of the in-plane magnetic correlations is related to the emergence of superconductivity in these heavy fermion compounds and could provide new insights in the description of unconventional superconductors.

- [1] J.D. Thompson & Z. Fisk, J. Phys. Soc. Japan 81, 11002 (2012).
- [2] D.M. Fobes *et al.*, J. Phys. Condens. Matter 29, 17LT01 (2017).
- [3] E.D. Bauer *et al.*, Phys. Rev. B 81, 180507 (2010).
- [4] N. Gauthier *et al.*, Phys. Rev. B 96, 064414 (2017).

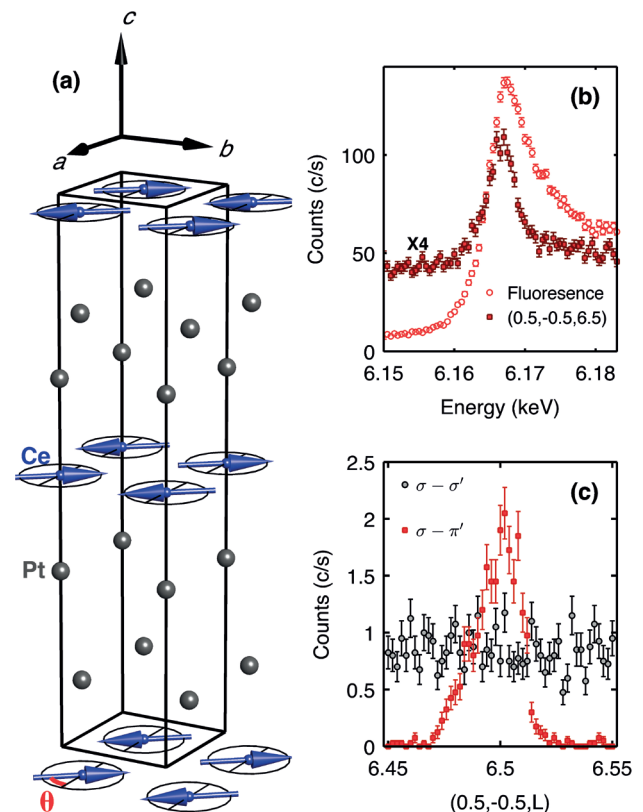


Fig. 13: (a) Magnetic structure of $CePt_2In_7$ at ambient pressure. The moments are collinear and lie in the basal plane. (b) Fluorescence at the Ce L_{II} absorption edge and the resonance of the magnetic scattering at the edge. (c) Polarisation analysis confirming the magnetic origin of the scattering in the channel $\sigma-\pi'$.

GIWAXS studies of organic field-effect transistors *in-operando*

O. Bikondoa, J. Kjelstrup-Hansen, M. Knaapila – for more information contact O. Bikondoa of XMaS, J. Kjelstrup-Hansen of the University of Southern Denmark or M. Knaapila of DTU Physics, Denmark.

oier.bikondoa@esrf.fr
 jkh@mci.sdu.dk
 matti.knaapila@fysik.dtu.dk

XMaS and Danish universities have recently demonstrated how organic field-effect transistors (OFETs) can be studied using GIWAXS* *in-operando* at XMaS. The device architecture is a bottom contact OFET with an interdigitated array of drain and source electrodes as shown in Fig. 14. The active layer is evaporated on top of the substrate leaving its surface open for surface sensitive GIWAXS which can be done simultaneously whilst electrically biasing the OFETs. The interdigitated electrodes are kept thin and the OFET channel width large to minimise background contributions from the electrodes and allow a large x-ray footprint yielding data with a good signal to noise ratio. These OFETs are also made compatible with ZIF-sockets, allowing direct integration into the MASDAR chamber on XMaS (Fig. 15).

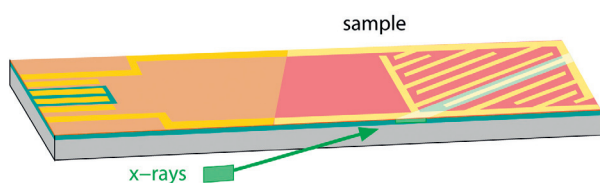


Fig. 14: Schematics of the experimental setting for GIWAXS measurements of OFETs *in-operando*.

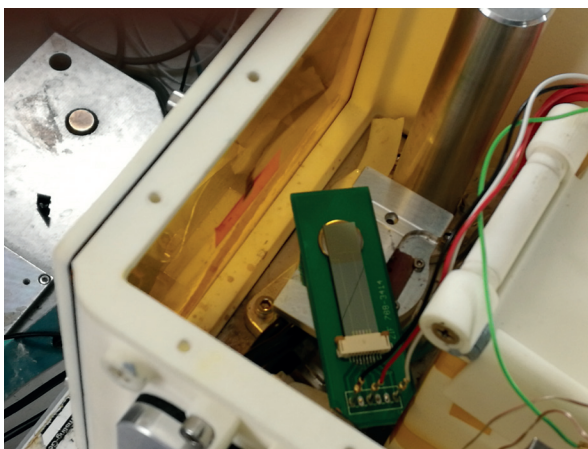


Fig. 15: Photo of a connected OFET in the MASDAR chamber.

This combination allows quick sample changes, reduces the air background and radiation damage and also protects OFET from moisture. The first GIWAXS measurements were made on OFETs based on naphthyl-end capped thiophene molecules (Fig. 16), which form p-type transistors. Long term measurements were also used to demonstrate the structural stability of this material class in operating transistors with the first results published in [1].

[1] M.K. Huss-Hansen *et al.*, *Org. Electron.* 49, 375 (2017).

* GIWAXS: Grazing Incidence Wide Angle X-ray Scattering

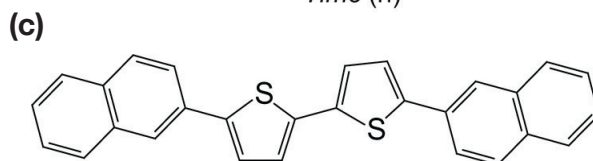
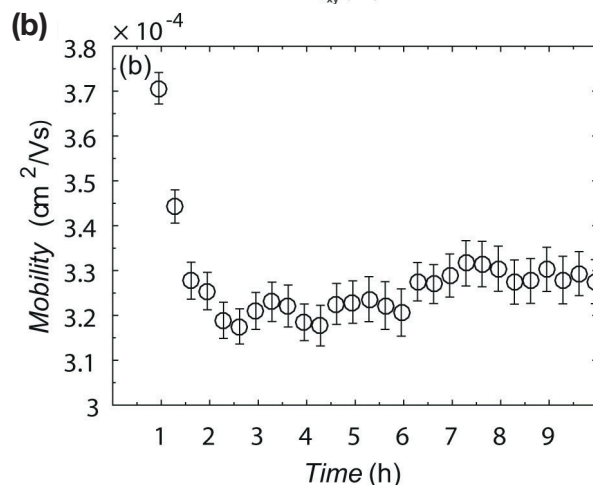
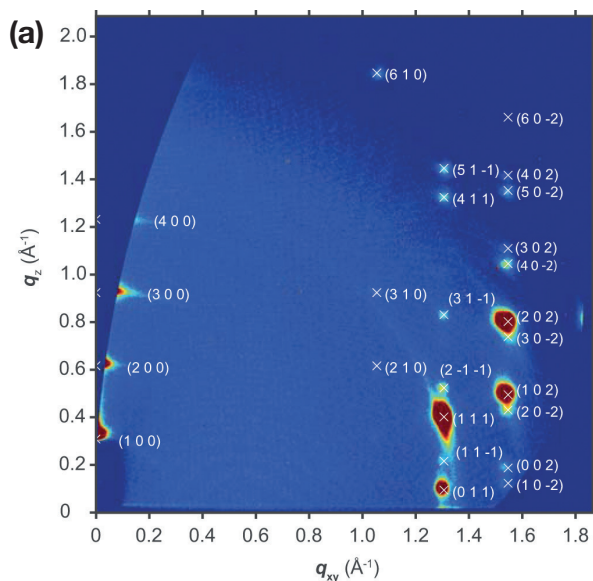


Fig. 16: (a) GIWAXS data from oligothiophene OFET and (b) simultaneously measured charge carrier mobility as a function of time. (c) Chemical structure of the studied material.

The twist bend nematic

W.D. Stevenson, X.B. Zeng, G. Ungar – for more information contact X.B. Zeng, Department of Materials Science and Engineering, University of Sheffield, UK.

x.zeng@sheffield.ac.uk

Over the last two decades exploration of a new liquid crystal phase, known as the twist bend nematic (NTB), has become a matter of great scientific interest. It is believed that in the NTB phase the local nematic director (average molecular direction) follows a helicoidal path, with a very short pitch length (~ 10 nm). This hypothesis, however, has proven difficult to unambiguously characterise, owing to the fact that the molecules inside it have no long range positional order, which means that helicity cannot be detected by normal x-ray scattering methods.

It was not until 2016 that the pitch length was first observed by resonant x-ray scattering (XRS) at the carbon absorption edge, using the fact the scattering at absorption edge becomes dependent on bond orientation; hence diffraction resulted from such orientation helicoids [1]. Unfortunately the experimental setup needed to use “soft x-rays” at the carbon edge has costly restrictions: It is difficult to incorporate external fields into the setup and no other scattering peaks of the NTB phase can be collected due to the extremely large wavelength of carbon edge (> 4 nm). This means that “soft x-ray” scattering studies are unable to provide answers to some of the deeper questions surrounding the NTB phase, which concern the packing behaviour and orientational order of the molecules.

In order to examine the chiral structure of the NTB phase and mitigate the restrictions of soft x-rays, we performed XRS at the selenium (Se) K-edge (12.658 keV) [2] in a Se-labelled sample synthesised by Dr. C. Welch and Prof. G.H. Mehl. Using XMaS at the ESRF, and I22 at DLS we were able to vary the incident x-ray energy and tune it to the Se K-edge, which lies in the “hard x-ray” regime. The use of higher energies permitted access to a much wider range of scattering angles, where information on the molecular packing is contained. Furthermore, the use of hard x-rays enabled us to align the samples using a magnetic field. At XMaS the 4 T superconducting magnet was used, with simultaneous temperature control. From such experiments, the first all-inclusive and well oriented small angle scattering pattern of the NTB phase was achieved (Fig. 17a). The experiments also showed how the orientational order

and the helical pitch length progressively reduce with temperature. Based on these and supporting grazing incidence studies also carried out at XMaS, molecular bend and tilt angles were obtained. The results demonstrate how even bent molecules (the unlikely nematogens) can, by adopting a small twist, still form a nematic liquid and a spiral through it. This leads to a molecule-level model of the NTB phase where molecules take a helical conformation and become segments of a helix, with the phase possessing helicoidal orientational order but no long range positional order. (Fig. 17b,c).

[1] C. Zhu *et al.*, Phys. Rev. Lett. 116, 147803 (2016).

[2] W.D. Stevenson *et al.*, Phys. Chem. Chem. Phys. 19, 13449 (2017).

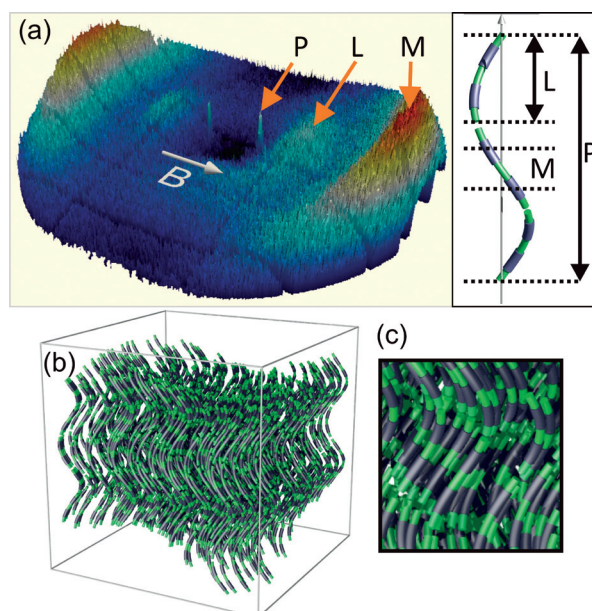


Fig. 17: (a) Surface plot of the 2D resonant scattering pattern of the NTB phase. The sharp peaks can be related to the helical pitch length (P) and the broad ones to average molecular spacings (M and L) along the local helical axis. (b) Model of the NTB phase with short range layering order. The layering is clearer in the close up in (c).

Effect of retained Cl on the Pd in ENCAT™ 30 catalysts: “*in-situ*” Pd L₃ and Cl K-edge XAFS

M.A. Newton, R. Nicholls, J. B. Brazier, B.N. Nguyen, C.J. Mulligan, K. Hellgardt, E.M. Barreiro, H. Emerich, K.K. Hii, I. Snigireva, P. Thompson – for more information contact M.A. Newton, ETH Zürich, Switzerland.

manewton68@gmail.com

Selective catalysis for fine chemicals synthesis using palladium is an extremely important and much researched field. Encapsulation of Pd acetate - ENCAT™30 - or small Pd(0) nanoparticles (NPs; ENCAT™30 NP) using polymer matrices has proved commercially successful for a range of catalytic conversions; the polymer encapsulation preventing the extremely problematic issue of the leaching of Pd into the reactant/product stream.

In studying the behaviour of these catalysts using Pd K-edge EXAFS* (SNBL, ESRF) we noticed a variability between different batches of ENCAT™30 NP [1, 2]. When heated under flowing ethanol/water solvents some batches readily produced Pd(0) NPs whereas others did not. Analysis of the Pd K-edge EXAFS suggested that in those that did not form Pd(0) NPs some Pd-Cl bonding was present. To further understand if and how Cl contamination might be affecting the Pd as well as how extensive this contamination was, we studied more batches of both ENCAT™30 and ENCAT™30 NP catalysts on XMaS [4]; the XMaS beamline allows us to address the Cl directly (Cl K-edge, 2.822 keV) as well as the

Pd (Pd L₃ edge, 3.174 keV) and provides the correct sample environment to study these systems in an *in-situ* manner [3].

Fig. 18 shows results obtained at the Cl K-edge that reveal aspects of the speciation of the Cl along with how these systems develop during heating in an aqueous ethanolic solvent flow to 350 K. These spectra, when referenced to the Pd L₃-edge XANES** (not shown) reveal that Cl can be present in very substantial amounts (Cl/Pd ≈ 1) and is not removed from the system through heating in the solvent. Further, the Cl K-edge pre-edge feature quantifies how much of this Cl is directly bonded to the Pd; such a pre-edge feature can only arise through direct binding of Cl to oxidised Pd centres. This shows that up to 40% of the Cl is bound to oxidised Pd centres in the starting ENCAT NP catalyst. Lastly we can see in the samples measured at 350 K (and in the native ENCAT 30 catalysts) a pronounced feature at 2.83 and 2.836 keV; this peak is due to the formation of NaClO₃ and NaClO₄ species. The corresponding Pd L₃ edge data confirms that in none of the starting samples is there any evidence for the Pd(0) that we should expect for ENCAT NP; even in the Pd(II) ENCAT30 samples we find evidence of direct Pd-Cl bonding albeit at a much lower level. Lastly it is evident that after heating in the flowing solvent, whilst the pre-edge feature is diminished it has not disappeared; Pd L₃ edge XAFS*** indicates that no more than 25% of the Pd is ever reduced to Pd(0) under the conditions applied when Cl is present.

Using the sample environment and low energy XAFS available at XMaS we have therefore demonstrated that substantial Cl contamination in these systems can result in severe modification of the behaviour of the Pd. The Cl results from the use of chlorinated solvents that can be encapsulated with the Pd and react with it. Direct Pd-Cl bonding then severely retards the formation of catalytically active Pd NPs. From these fundamental measurements we have therefore gained valuable insight into how changing a commercial process to avoid the use of chlorinated solvents should result in a more consistent product that can readily yield the catalytically active Pd nanoparticles that ENCAT30 NP was originally designed to produce.

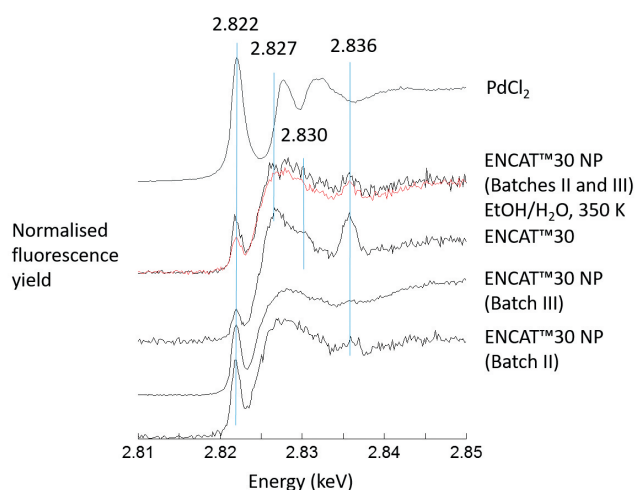


Fig 18: Cl K-edge XANES derived from ENCAT Pd catalysts as received and after heating in flowing aqueous ethanol. A spectrum due to PdCl₂ is also given.

[1] C. Ramarao *et al.*, Chem. Commun.10, 1132 (2002).

[2] S.V. Ley *et al.*, Chem. Commun. 10, 1134 (2002).

[3] S.V. Ley *et al.*, Org. Letts. 5, 4665 (2003).

[4] M.A. Newton *et al.*, Catal. Struct. React. 3, 149 (2017).

* EXAFS: Extended X-ray Absorption Fine Structure

** XANES: X-ray Absorption Near Edge Spectroscopy

*** XAFS: X-ray Absorption Fluorescence Spectroscopy

Carbon nanotubes as templates for 1D nanostructures via a one-reactant-one-pot method

C.T. Stoppiello, J. Biskupek, Z.Y. Li, G.A. Rance, A. Botos, R.M. Fogarty, R.A. Bourne, J. Yuan, K.R.J. Lovelock, P. Thompson, U. Kaiser, T.W. Chamberlain, A.N. Khlobystov – for more information contact T.W. Chamberlain, iPRD, School of Chemistry, University of Leeds, U.K.

t.w.chamberlain@leeds.ac.uk

Harnessing functional properties which emerge at the nanoscale is the key to developing superior materials for catalytic, electronic and biomedical applications. The internal cavity of single-walled carbon nanotubes (SWNTs) provides an effective template for control of the exact positions and orientations of molecules and atoms and has been successfully applied to the construction of nanoscale architectures from a variety of metals,¹⁻³ organic molecules, and inorganic compounds [1]. Low-dimensional inorganic materials, including transition metal chalcogenides, are of particular interest as their semiconducting properties can be precisely tuned by shaping their structures into nanoribbons. While the host-nanotube can control the dimensions of the inorganic structure, the stoichiometry is much more difficult to control.

An all-in-one molecular precursor that contains all the necessary elements in correct proportion for the desired inorganic product, encapsulated in SWNTs and subsequently converted into the inorganic material offers a highly effective solution to this challenge. The one-pot-one-reactant synthesis involves a single step so that the stoichiometric ratio of the metal and halogen/chalcogen in the resultant material can be precisely controlled [2]. The insertion of complexes of transition metals with ligands containing the required non-metallic elements into SWNTs is illustrated for platinum compounds containing Pt:I and Pt:S in ratios of 1:2.

The L_{III} edge of Pt (measured in FDXAS at XMaS) can be used as a probe of the oxidation state of the species inside the nanotube and can thus elucidate any transfer of electron density to or from the reactant to the nanotube upon encapsulation. Furthermore, the characteristic G-band, ubiquitously observed in the Raman spectra of graphitic nanostructures, is sensitive to strain and curvature of the nanotube, and can be used to measure any electron transfer from the nanotube to guest molecules. Interestingly, the encapsulation of platinum $Pt(acac)_2I_2@SWNT$ led to a significant reduction in the absorption energy of the Pt L_{III} edge indicative of an increase of electron

density onto the Pt centre as compared to free $Pt(acac)_2I_2$, (Fig. 19). This is complemented by a significant blue shift of the Raman G-band of the host SWNT, implying electron transfer from the nanotube to the guest molecule. In contrast, $Pt(acac)_2(SCN)_2@SWNT$ showed a decrease in the Pt edge energy in the FD-XAS and a red shift of the nanotube G-band, indicating that electron density is transferred in the opposite direction, i.e. from $Pt(acac)_2(SCN)_2$ to SWNTs. Thermal treatment led to the facile transformation of the molecular precursors to the desired inorganic structures, $PtI_2@SWNT$ or $PtS_2@SWNT$, with a nearly 1:2 stoichiometric metal to halogen/chalcogen composition and nanowire morphology.

AC-HRTEM^{††} imaging reveals that the atomic level structure of the $PtI_2@SWNT$ is different to that of the bulk (Fig. 19), with high-coordinated I-atoms in the middle of the structure and low-coordinated I atoms located in the space between Pt and SWNT wall, despite the overall Pt:I ratio being the same as in the bulk crystal. In contrast, in $PtS_2@SWNT$ the nanowire adopts a hexagonal lattice similar to bulk PtS_2 .

[1] A. Botos *et al.*, J. Am. Chem. Soc. 138, 8175 (2016).

[2] C.T. Stoppiello *et al.*, Nanoscale 9, 14385 (2017).

* FD-XAS: Fluorescence Detected X-ray Absorption Spectroscopy

** AC-HRTEM: Aberration Corrected High Resolution Transmission Electron Microscopy

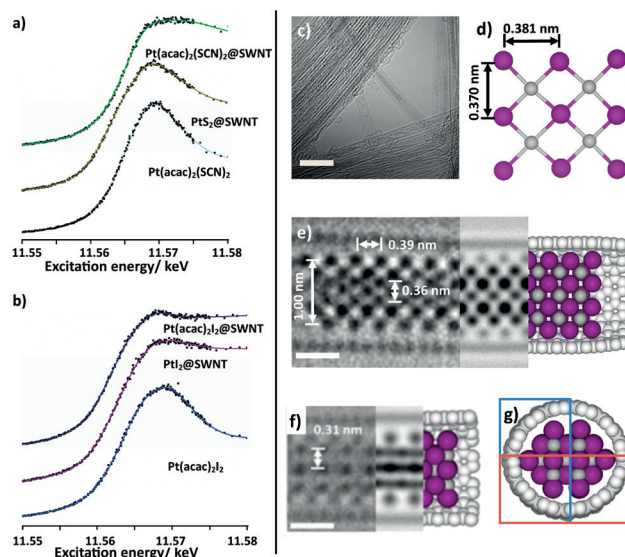


Fig. 19: (a) and (b) FD-XAS showing the Pt L_{III} edge of materials formed in SWNTs. (c) AC-HRTEM image showing a bundle of $PtI_2@SWNT$, the scale bar is 5 nm; (d) an extended portion of the crystal structure of PtI_2 derived from the asymmetric unit of bulk PtI_2 ; (e,f,g) two AC-HRTEM micrographs showing $PtI_2@SWNT$ in different projections, accompanying HRTEM simulations and computational models, the scale bars are 0.5 nm.

Access to offline facilities

→ Our website

This can be found at: www.xmas.ac.uk and contains the definitive information about the beamline and offline facilities, future and past workshops, press articles as well as current Key Performance Indicators (KPIs). You can also follow what happens on the beamline every week on [Twitter@XMaSBeam](https://twitter.com/XMaSBeam).

→ Application for offline time

Submit your application directly on the XMaS web site.

www.xmas.ac.uk

Select “**XMaS Offline Facilities**” and then
“**Application for Offline Facilities**”

Follow the instructions carefully. Do not forget to load your 1-2 page proposal at the end of the application form. XMaS will provide travel and subsistence for only 1 user. Note that users will be allowed in the ESRF experimental hall until December 2018 which is the official start of the ESRF EBS shutdown. During the dark period (December 2018 – August 2020), the XMaS staff may have to handle remote or “mail in” applications as user access to the ESRF will likely to be restricted. Please contact the local staff listed below to discuss any potential experiments.

Users coming to use the offline facilities will be entitled to €70 per day – the equivalent actually reimbursed in pounds sterling. Offline proposals will be run as in-house experiments. Laurence Bouchenoire (bouchenoire@esrf.fr) will complete the Safety form with information supplied in your application form as well as arrange the site passes and any accommodation that may be required. The ESRF guest house still appears adequate to accommodate all our users, though CRG users will always have a lower priority than the ESRF’s own users.

→ Beamline people

● **Beamline Responsible** – Didier Wermeille (didier.wermeille@esrf.fr), in partnership with the Directors, oversees the activities of the user communities as well as the programmes and developments that are performed on the beamline. He is also the beamline Safety Representative.

● **Beamline Coordinator** – Laurence Bouchenoire, (bouchenoire@esrf.fr), looks after beamline operations and can provide you with general information about the beamline, application procedures, scheduling, etc. Laurence should normally be your first point of contact.

● **Beamline Scientists** – Didier Wermeille (didier.wermeille@esrf.fr), Oier Bikondoa (oier.bikondoa@esrf.fr), Laurence Bouchenoire (bouchenoire@esrf.fr) and Simon Brown (sbrown@esrf.fr) are Beamline Scientists and will provide local contact support during experiments. They can also assist with queries regarding data analysis and software.

● **Technical Support** – Paul Thompson (pthomps@esrf.fr) is the contact for instrument development and technical support. He is assisted by John Kervin (jkervin@liv.ac.uk), who is based at the University of Liverpool. He provides further technical back-up and spends part of his time on-site at XMaS.

● **Project Directors** – Chris Lucas (clucas@liv.ac.uk) and Tom Hase (t.p.a.hase@warwick.ac.uk) continue to travel between the UK and France to oversee the operation of the beamline.

Malcolm Cooper (m.j.cooper@warwick.ac.uk) remains involved in the beamline operation as an Emeritus Professor at the University of Warwick. Natacha Borrel (n.borrel@warwick.ac.uk) is the administrator on the project and is based in the Department of Physics at Warwick. All queries regarding expenses claims, etc. should be directed to her.

→ The Project Management Committee

The current membership of the committee is as follows:

- P. Hatton (chair), University of Durham
- K. Bowman, EPSRC
- S. Beaufoy, University of Warwick
- A. Boothroyd, University of Oxford
- M. Cain, Electrosiences Ltd
- R. Cernik, University of Manchester
- K. Edler, University of Bath
- B. Hickey, University of Leeds
- S. Langridge, ISIS, Rutherford Appleton Laboratory
- C. Nicklin, Diamond Light Source
- W. Stirling, Institut Laue Langevin

in addition to the above, the directors, the chair of the Peer Review Panel, the CRG Liaison A. Kaprolat and the beamline team are in attendance at the meetings which happen twice a year.

→ The Peer Review Panel

The current membership of the panel is as follows:

- R. Johnson (chair), University of Oxford
- E. Blackburn, University of Birmingham
- W. Briscoe, University of Bristol
- S. Corr, University of Glasgow
- C. Detlefs, ESRF
- Y. Gründer, University of Liverpool
- J. Quintanilla, University of Kent
- R. Walton, University of Warwick
- J. Webster, ISIS

In addition either Chris Lucas or Tom Hase attends their meetings in an advisory role.

PUBLISH PLEASE!!... and keep us informed

Although the list of XMaS papers is growing we still need more of those publications to appear. We ask you to provide Natacha Borrel with the reference and DOI code. You can also submit the reference of your new publication directly from our web site (<https://tinyurl.com/yclguqdh>).

IMPORTANT!

It is important that we acknowledge the support from EPSRC in any publications. When beamline staff have made a significant contribution to your scientific investigation you may naturally want to include them as authors. Otherwise we ask that you add an acknowledgement, of the form:

“**XMaS is a UK national facility supported by EPSRC. We are grateful to all the beam line team for their support.**”



is an EPSRC sponsored project